



Case report

Comparing fundus autofluorescence and infrared imaging findings of peripheral retinoschisis, schisis detachment, and retinal detachment



Natalie T. Huang^a, Catherine Georgiadis^b, Jessica Gomez^c, Peter H. Tang^d, Paul Drayna^e, Dara D. Koozekanani^f, Frederik J.G.M. van Kuijk^f, Sandra R. Montezuma^{f,*}

^a Department of Ophthalmology, SUNY Upstate Medical University, Syracuse, NY, USA

^b Department of Ophthalmology, Hennepin County Medical Center, Minneapolis, MN, USA

^c San Diego Retina Associates, San Diego, CA, USA

^d Vitreoretinal Surgery, P.A., Edina, MN, USA

^e Wilford Hall Eye Center, Lackland Air Force Base, San Antonio, TX, USA

^f Department of Ophthalmology and Visual Neurosciences, University of Minnesota, Minneapolis, MN, USA

ARTICLE INFO

Keywords:

Retinoschisis
Retinal detachment
Schisis detachment
Fundus autofluorescence
Infrared imaging
Spectral domain optical coherence tomography

ABSTRACT

Purpose: The primary goal of this study was to identify characteristic features of peripheral degenerative retinoschisis (RS), schisis detachment (SD) and retinal detachment (RD) on both fundus autofluorescence (FAF) and infrared (IR) imaging, using spectral domain optical coherence tomography (SD-OCT) imaging of the peripheral retina as the confirmatory imaging tool.

Methods: This is a descriptive case series study. A total of 27 eyes of 22 patients were included. Thirteen eyes of 10 patients diagnosed with RS, 4 eyes of 3 patients diagnosed with SD, and 10 eyes of 9 patients diagnosed with RD were included. Patients with images of poor quality were excluded. Heidelberg Spectralis HRA + OCT machine (Heidelberg Engineering, Heidelberg, Germany) were used to acquire the images.

Results: All conditions appeared as areas of hypo-AF on FAF and hypo-reflectance on IR imaging. Accentuated vasculature of the lesion was noted with IR imaging due to elevation of the RS and RD, which was less frequently observed with FAF. On FAF, a hyper-AF leading edge around the RS lesion indicated the presence of intraretinal or subretinal fluid and an extension of the RS. Retinal breaks/holes were best visualized with IR imaging. SD-OCT confirmed the diagnosis in all performed cases.

Conclusions: We were unable to differentiate between RS and RD based solely on findings from FAF and IR imaging. However, the combination of them with SD-OCT can assist in the diagnosis of RS from RD and in the evaluation of RS progression. OCT remains the main modality imaging to differentiate these conditions.

1. Introduction

Traditionally, differentiating between peripheral degenerative retinoschisis (RS) and retinal detachment (RD) relied heavily upon clinical features observed on the fundus through biomicroscopy and ultrasound imaging. RS lesions tend to have a smooth domed shape with an absence of hemorrhage, pigmentation, or shifting fluid, with laser photocoagulation uptake.¹ By contrast, RD lesions appear to have a corrugated surface, with variable shifting fluids and a relative scotoma, but does not uptake laser photocoagulation.¹ Recent advancements in fundus autofluorescence (FAF) and infrared (IR) imaging have enhanced our diagnostic imaging capabilities. FAF allows for topographical mapping of lipofuscin distribution within the retinal pigment epithelium (RPE) as well as other fluorophores that may occur in

diseases of the outer retina and subretinal space.² It relies on the photoexcitation of fluorophores to produce autofluorescence.³ IR imaging uses near-infrared light to evaluate the RPE and underlying choroidal structures. Due to its longer wavelength, IR imaging has improved penetration through media opacities compared to fundus photography (FP) for visualizing retinal pathology.⁴

The primary goal of this study was to identify features on both FAF and IR imaging of RS, schisis detachment (SD) and RD, using spectral domain optical coherence tomography (SD-OCT) imaging of the peripheral retina as the confirmatory imaging tool. Images from these respective modalities were compared to those obtained with standard FP. In recent literature, there have been studies that reported the imaging characteristic differences between RS and RD using wide-field infrared imaging,⁵ SD-OCT⁶⁻⁹ and ultra-wide-field steering-based SD-OCT.¹⁰ In

* Corresponding author. 420 Delaware Street SE, MMC 493, Minneapolis, MN, 55455, USA.

E-mail address: smontezu@umn.edu (S.R. Montezuma).

<https://doi.org/10.1016/j.ajoc.2020.100666>

Received 10 July 2018; Received in revised form 3 October 2019; Accepted 11 March 2020

Available online 26 March 2020

2451-9936/© 2020 The Authors. Published by Elsevier Inc. This is an open access article under the CC BY-NC-ND license

(<http://creativecommons.org/licenses/by-nc-nd/4.0/>).

our study, we reviewed and compared both FAF findings and IR imaging to evaluate the strengths of using either modality in diagnosing RS and RD.

2. Materials and methods

This was a descriptive observational case series study. The study adhered to the principles of the Declaration of Helsinki and was approved by the Institutional Review Board of the University of Minnesota. Signed informed consent documentation was obtained from all participants. Patients who presented to the University of Minnesota Department of Ophthalmology and Visual Neurosciences and were diagnosed clinically with peripheral RS, SD, or RD were invited to participate in the study. All participants underwent FP, FAF, IR imaging and OCT. FP was performed using a Topcon Fundus Camera (50DX Model). FAF and IR imaging were obtained using a Heidelberg Spectralis® HRA + OCT with 102 and 55-degree non-contact lenses, respectively. Macular and peripheral SD-OCT was also obtained using the Heidelberg Spectralis® HRA + OCT. In addition, some patients underwent Optos fundus color and Optos FAF when it became available in July, 2015 in our institution (Optos, Inc., Malborough, MA, USA). The study was conducted from Summer 2013 to Summer 2015. Patients with poor image quality were excluded from the study.

3. Results

The study included 27 eyes (16 right eyes [OD], 11 left eyes [OS]) of 22 patients (15 males and 7 females), aged from 19 to 79 years (mean age of 54.2 years). RS was diagnosed in 13 eyes (8 OD, 5 OS) of 10 patients. Mixed RS and SD were seen in 4 eyes of 3 patients. RD was identified in 10 eyes (6 OD, 4 OS) of 10 patients, of which 7 were Rhegmatogenous, 2 were tractional, 1 was serous, and one eye displayed both RS and RD. The duration of RS ranged from newly diagnosed to more than 16 years RS was found predominantly inferotemporally (8/13 eyes), with the rest located superotemporally (5/13 eyes). RD was primarily located superotemporally.

On FAF, all of the lesions of RS and SD, and 9/10 RD lesions appeared as hypo-AF. A hyper-AF leading edge was seen in 3/13 eyes with RS, in 1/4 eyes with SD, and in 2/10 eyes with RD. OCT of the areas with hyper-AF leading edge demonstrated either low-lying schisis (Figs. 1D and E, 3D) or shallow detachment (Figs. 3E and 4C). On IR imaging, 11/13 of RS, 4/4 SD and 9/10 RD lesions appeared as well delineated areas of hypo-reflectance. A hyper-reflective leading edge along the sharply demarcated areas of hypo-reflectance was present in 4/13 RS, 1/4 SD and 1/10 RD lesions, which corresponded to a shallow RS or SRF on OCT (Figs. 1, 4 and 5). Accentuated retinal vasculature on IR imaging was evident in 11/13 RS, 3/4 SD and 5/10 RD lesion eyes. Retinal tears/holes were demonstrated in 2/13 RS, 1/4 SD and 3/10 RD lesions on IR imaging. Retinal holes were visualized in 1/13 with RS and in 1/4 with SD on FAF. The different features of RS, SD, and RD found on FAF and IR imaging were summarized in Table 1. We found a hyper-reflective leading edge along the sharply demarcated areas of hypo-reflectance from large RS or RD. In these eyes, OCT through the region confirmed that a shallow RS or SRF extended past the hypo-reflectance demarcation line into an area of hyper-reflectance.

3.1. Retinoschisis

FP, FAF, and IR imaging, and OCT imaging of one eye diagnosed with RS are shown in Fig. 1. Compared to FP, it was easier to delineate the border of the lesion on FAF and IR imaging. Both FAF (Fig. 1B) and IR imaging (Fig. 1C) showed accentuated vasculature. OCT images (Figs. 1D and E) of the edge of lesion demonstrated an extended low-lying RS, which is shown as a hyper-reflective leading edge on IR Imaging (Fig. 1C). FAF and IR imaging of two eyes diagnosed with RS, and one eye with SD (Fig. 2C and D), confirmed with OCT, were shown

in Fig. 2. On FAF (Fig. 2 A, C & E), the region of RS appeared as a well-demarcated area of hypo-AF of different patterns, ranging from patchy (Fig. 2A), confluent (Fig. 2C) to granular (Fig. 2E), with a hyper-AF leading edge that was either well-defined (Fig. 2C) or patchy. The intensity of the lesion varied from mild (Fig. 2E), moderate to intense (Fig. 2 A & C). On IR imaging (Fig. 2 B, D & F), areas of RS appeared as well-delineated areas of hypo-reflectance with accentuated vasculature (Fig. 2F) in some cases. Inner and outer retinal holes (Figs. 2B & 3D) were well visualized. Nine of 10 patients who returned to follow up demonstrated no progression of RS lesions based on the combination of IR imaging, FAF and OCT. The average follow-up duration for these patients was 30 months.

3.2. Case study

A series of FAF and IR imaging were obtained on a patient with RS that was progressed to SD over time (Fig. 3). The patient was first diagnosed with a large superior RS OD clinically and on IR imaging and color FP (Fig. 3A and B) in October 2013, which was confirmed with OCT (Fig. 3C). A few months later, a new outer retinal hole was visualized on IR imaging (Fig. 3D) but not on FAF (Fig. 3E), while OCT re-demonstrated a RS (Fig. 3D–F). Eventually, the outer hole was noted to be enlarged on IR imaging (Fig. 3G) and a SD (Fig. 3I) was noted on OCT. Laser retinopexy was recommended, but the patient deferred. Four months later, the SD was observed to have progressed. An Optos FAF-guided laser retinopexy was then performed, and the lesion was stabilized (Fig. 3J–L).

3.3. Schisis detachment

FAF and IR imaging of one eye diagnosed with SD, confirmed with OCT, are shown in Fig. 4. The lesion had been treated with barrier laser retinopexy at the edges. Similar to the findings of RS on FAF, the lesion appeared as an area of confluent hypo-AF, with a relative hyper-AF leading edge between the laser scars and the dark border of the lesion (Fig. 4B), corresponding to an area of low-lying SD. On IR imaging (Fig. 4C), accentuated vasculature and hypo-reflectance with a clear demarcation line were noted. OCT images (Fig. 4D and E) of the edges of the lesions demonstrated a low-lying RS and a shallow SD. All four patients were followed clinically and the average follow up duration was 53 months. One patient had a slow progression of SD based on OCT imaging and was treated with laser retinopexy. Three other patients remained clinically stable.

3.4. Retinal detachment

Images acquired from one eye with RD using FAF, IR imaging, and OCT are displayed in Fig. 5. Compared to FP, both FAF and IR imaging demonstrated sharper delineation of the lesion with area of hypo-AF (Fig. 5B) and hypo-reflectance (Fig. 5C), respectively. OCT imaging (Fig. 5C') across the edge of hyper-reflective leading edge on IR imaging revealed a shallow RD with subretinal fluid. Four of the 9 patients subsequently showed no changes in their RD lesions based on IR, FAF and OCT imaging. The average duration of follow up on these patients was 17 months.

4. Discussion

The results of our study highlight the importance of the combined use of FAF, IR and OCT imaging in diagnosing and monitoring RS, SD, and RD lesions.

4.1. FAF

Most peripheral RS were shown as an area of confluent hypo-AF with moderate intensity FAF. The difference in the intensity of hypo-AF

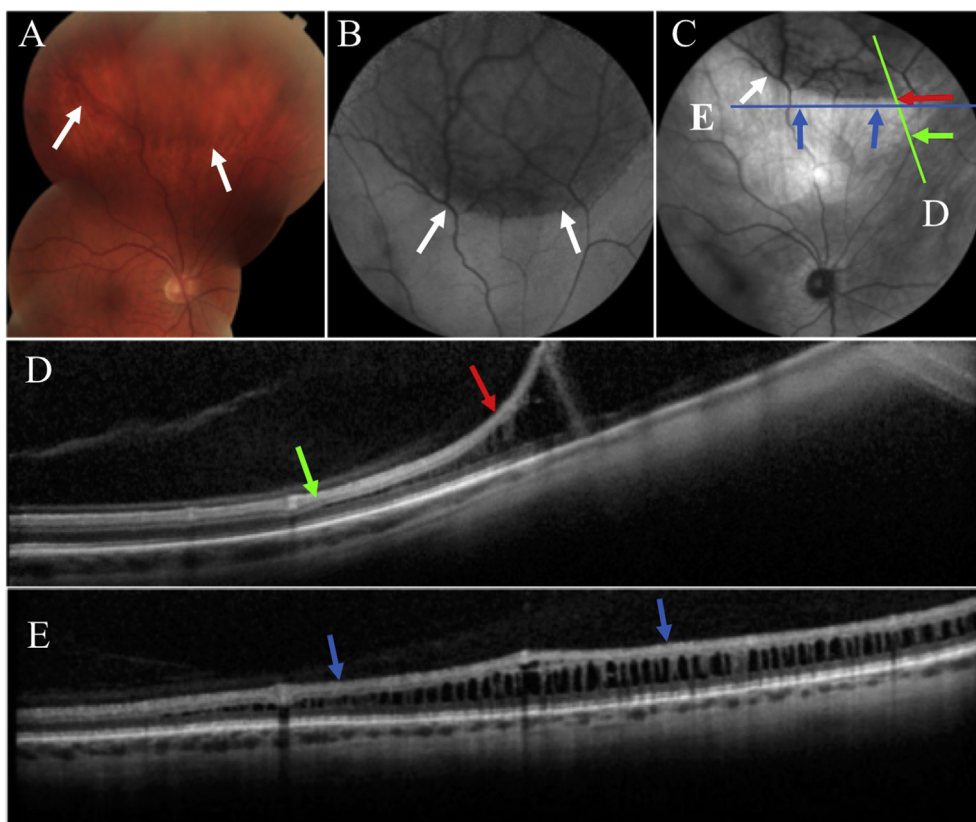


Fig. 1. Characterization of retinoschisis on multiple imaging modalities. Patient with retinoschisis underwent imaging with FP (A), FAF (B), and IR imaging (C). Note the difficulty in discerning the edge of retinoschisis in FP, which is better shown in both FAF and IR imaging (white arrows). OCT scan indicated by green line in C is shown (D), highlighting that retinoschisis extends along the hyper-reflective signal (green arrow) past the hypo-reflectance border (red arrow). OCT scan indicated by blue line in C is shown (E), demonstrating low-lying retinoschisis (blue arrows) in the hyper-reflective leading edge of the lesion. (For interpretation of the references to color in this figure legend, the reader is referred to the Web version of this article.)

is unclear. We hypothesize that it could be either related to the degree of elevation of the RS or RD or it may be caused by the variation in detector gain set by the photographer to maintain the exposure. The appearance of peripheral RDs as hypo-AF, and retinal breaks as hyper-AF on FAF, along with a hyper-AF leading edge around the detachment was previously reported by Salvanos et al.¹¹ Although the significance of this hypo-AF appearance is unknown, we hypothesize that it may suggest underlying structural changes ultimately manifested as metabolic changes in the photoreceptor/RPE layer.

A hyper-AF leading edge was observed in some lesions, which were found to have extended low-lying RS, SD, or shallow RD. This was previously noted to be an area of shallow subretinal fluid (SRF) on OCT by Witmer et al.¹² The significance of a hyper-AF leading edge found on FAF is not completely clear. It is hypothesized that the increased levels of AF may indicate an accumulation of fluorophores within the subretinal fluid along with the presence of oxidative stress and increased metabolic activity as the RPE enters a pre-apoptotic state.^{11–13} Another source of hyper-AF could be the presence of macrophages containing pigment granules in the subretinal fluid.¹⁴

Treatment options for SD are at the surgeon's discretion. When laser

retinopexy is used, the hyper-AF leading edge can serve as a landmark not only for the surgeon to demarcate the edges of the lesion and place the laser spots safely but also for further monitoring of the lesion after therapeutic laser retinopexy. It will be useful to evaluate if there is an incomplete treatment or progression of the RD.

4.2. IR imaging

On IR imaging, areas of peripheral RS, SD, and RD appeared as well-delineated areas of hypo-reflectance with an occasional hyper-reflective leading edge. The hypo-reflectance of the bullous RS lesions was most likely due to their oblique orientation towards the camera, and the inner retinal surface reflects the illuminating light away from the camera, hence the region seems darker. The same optical effect might also explain why the lesion appears hypo-AF on FAF. The accentuated vasculature, observed in all three types of lesions on both FAF and IR imaging, was caused by the elevation of the lesion which brought the vessels closer to the camera, hence magnified the vessels in the lesion compared to the rest of the vessels on the attached retina. The extension of these accentuated vessels can serve as another landmark for lesion

Table 1

Fundus autofluorescence (FAF) and Infrared (IR) imaging features of retinoschisis, schisis detachment, and retinal detachment.

Imaging Modality	Imaging characteristics	Retinoschisis	Schisis detachment	Retinal detachment
FAF	Well demarcated areas of hypo-AF	13/13	4/4	9/10
	Definite hyper-AF leading edge	3/13	1/4	2/10
	Accentuated vasculature	5/13	1/4	2/10
	Visible tears, holes and breaks	1/13	1/4	0/10
IR Imaging	Well delineated area of hypo-reflectance	12/13	4/4	9/10
	Definite hyper-reflective leading edge	4/13	1/4	1/10
	Accentuated vasculature	11/13	3/4	5/10
	Visible tears, holes and breaks	2/13	1/4	3/10

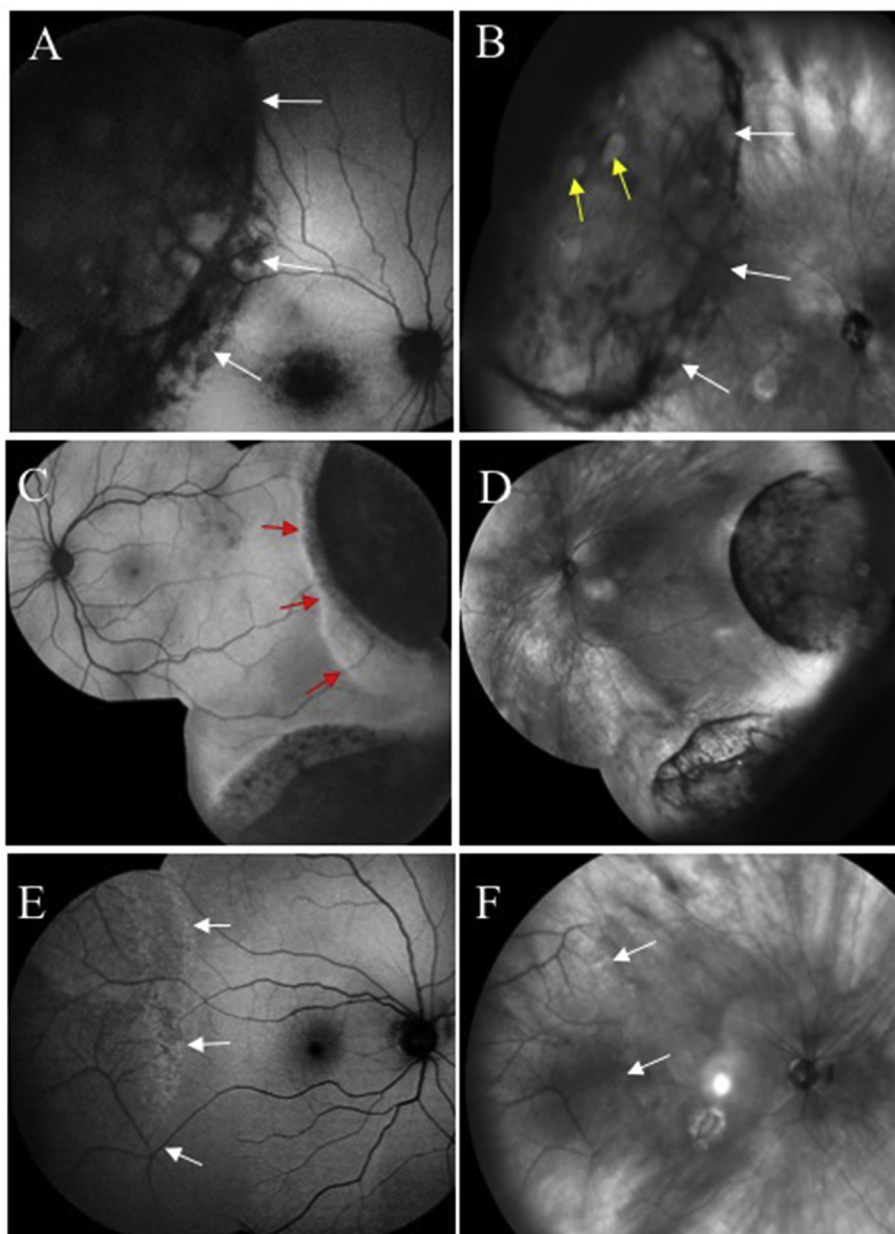


Fig. 2. Comparison of retinoschisis on FAF (left column) and IR imaging (right column). On FAF (A, C, E), three patterns of retinoschisis were observed, including patchy (A), confluent (C), and granular (E). Furthermore, intensity of hypo-AF varied among different retinoschisis patterns ranging from mild (E) to intense (A & C). A well-defined hyper-AF leading edge of retinoschisis (C) was observed. On IR imaging (B, D, F), areas of retinoschisis display hypo-reflectance and increased vascular prominence (F). Outer retinal holes (B) are visualized in retinoschisis on IR imaging. White arrows indicate borders of retinoschisis, red arrows indicate a hyper-AF leading edge, and yellow arrows indicate retinal holes. (For interpretation of the references to color in this figure legend, the reader is referred to the Web version of this article.)

progression over time.

We also noted that a hyper-reflective leading edge on IR imaging, although this was less defined than a hyper-AF leading edge in FAF. This differed from the findings made by Witmer and Salvano.^{11,12} We surmise that the hyper-reflective leading edge of RS observed on IR imaging is due to the vertically oriented cystic space of the low-lying RS at the lesion edge, which allows for a clear window through which to view the RPE; therefore, appearing brighter on imaging.

One significant observation gained from our study is that IR imaging is a superior modality for visualizing retinal vasculature, tears, holes and breaks, which is helpful in surgical planning and patient education.

In general, the majority of RS lesions appeared as areas of hypo-AF on FAF and hypo-reflectance on IR imaging. As previously described in the literature, these findings are likely due to blocking of AF and IR signals by subretinal and intraretinal fluid.^{11,15,16} SD-OCT helps to confirm RS, SD or RD; however, it could be less useful in delineating the extension of the RS or RD and for assessing progression without having the IR and FAF images. In addition, it is technically more challenging to obtain consistent extramacular OCT imaging than FAF or IR imaging on

the peripheral retina for long-term follow-up, as OCT is more dependent upon skillful photographers as well as patient's precise positioning for consistent results, particularly in institutions where ultra-wide-field steering-based SD-OCT is not available.

Our study was limited due to the small sample size and that Optos AF was used late in the study, therefore, the Optos images were not used for data analysis. Also, only a small portion of the patients followed up regularly throughout this two-year study, which limited the use of three modes of imaging for monitoring progression of lesions. Finally, the use of peripheral OCT requires cooperation of the patient and a skillful photographer to maintain the same angle during each study, which affected its consistency as a gold standard for monitoring lesion progression.

In conclusion, the combination of FAF, IR imaging, and SD-OCT, along with clinical findings found on fundus examination with scleral depression are helpful in diagnosing, monitoring and managing RS, SD, and RD. OCT however remains the main modality imaging to differentiate these conditions. In the future, the use of ultra-widefield OCT and peripheral OCT images will allow better diagnostic accuracy of

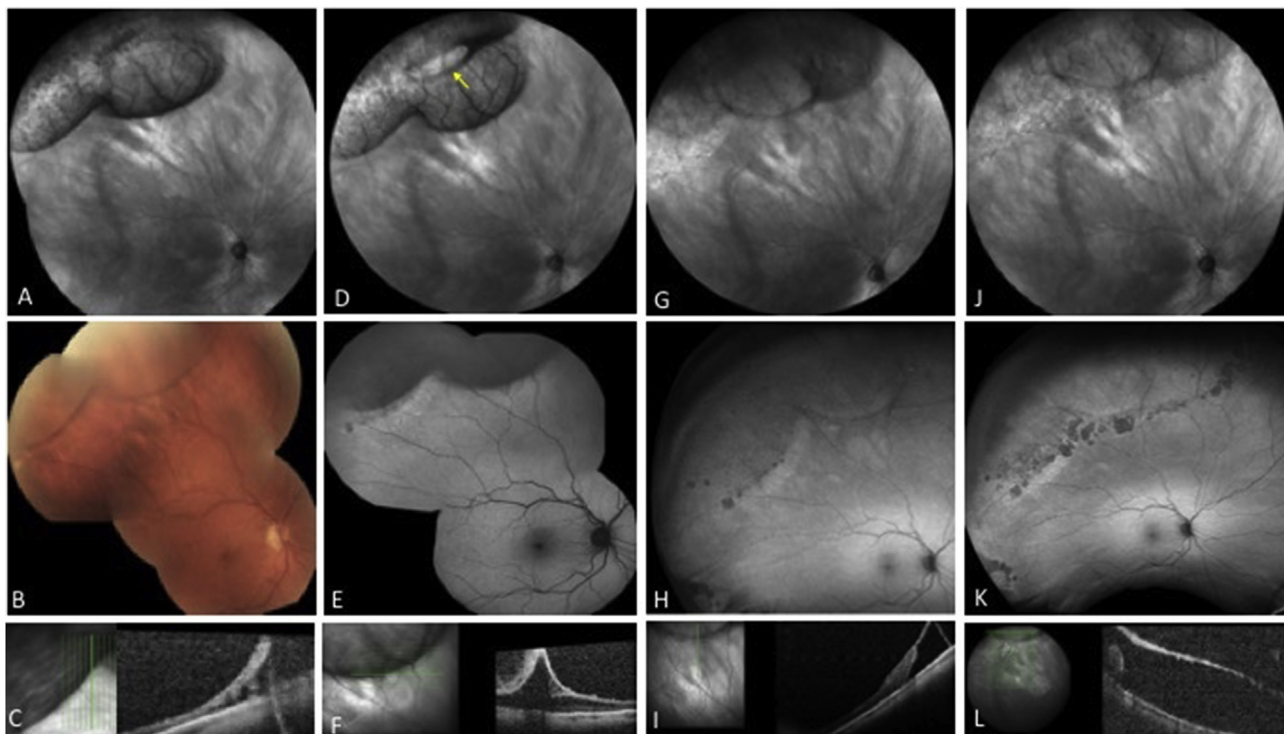


Fig. 3. Multimodal imaging follow up on one case of retinoschisis that progressed to schisis detachment. A-C Retinoschisis Diagnosed with Infrared (IR) imaging (A), color funduscopy (B) and OCT (C); D- F were taken two months later, with a new retinal outer hole (yellow arrow) visualized on IR imaging (D) only and not on AF (E) while OCT still shows retinoschisis (F); G-I were images taken in a two-month following the previous (D-F) with an enlarging retinal hole (double yellow arrows) demonstrated on IR imaging (G). The AF images shown in H and K were taken by Optos. OCT at this time showed progression to a schisis detachment (I). Four months later, Optos AF (K) guided laser retinopexy were employed to stabilize the Retinoschisis lesion. IR imaging (J) and OCT (L) demonstrated chronic enlarged retinoschisis. (For interpretation of the references to color in this figure legend, the reader is referred to the Web version of this article.)

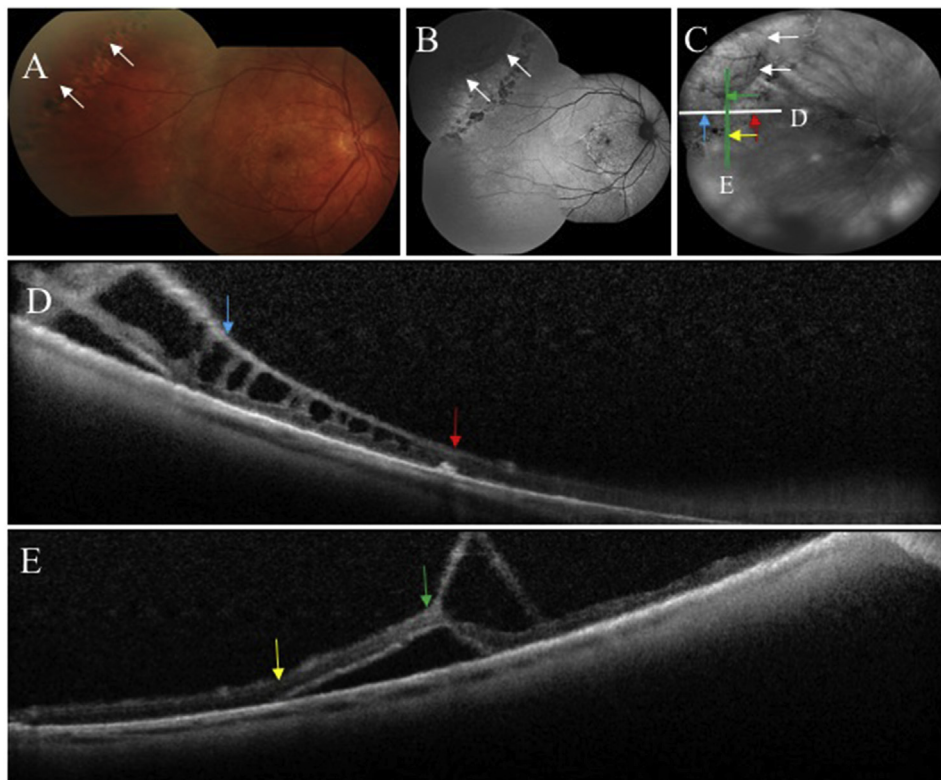


Fig. 4. Characterization of schisis detachment on multiple imaging modalities. A schisis detachment shown on FP (A), FAF (B), IR imaging (C), and OCT (D & E) after laser retinopexy. Horizontal (D) and vertical (E) OCT of the lesion edge demonstrated the hyper-reflective leading edge as low-lying retinal schisis (between blue and red arrows) or schisis detachment (between yellow and green arrows). (For interpretation of the references to color in this figure legend, the reader is referred to the Web version of this article.)

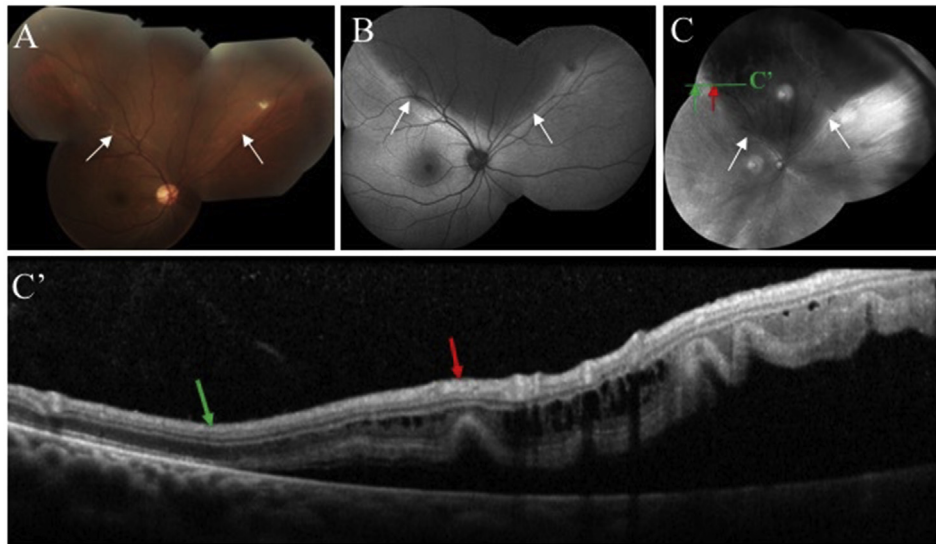


Fig. 5. Characterization of retinal detachment on multiple imaging modalities. A bullous retinal detachment demonstrated on FP (A), FAF (B), IR imaging (C), and OCT (C'). Note the contours of the bullous retinal detachment on FP are better visualized on FAF and IR imaging (white arrows). OCT scan indicated by green line in C is shown (C'). The hyper-reflective leading edge on IR imaging was shown as low-lying retinal detachment shown between the green arrow and red arrow. (For interpretation of the references to color in this figure legend, the reader is referred to the Web version of this article.)

identifying and differentiating RS, SD and RD.

Patient consent

The study was approved by the Institutional Review Board of the University of Minnesota. Written informed consent for the research was obtained from the patients and the study was conducted in accordance with HIPAA regulations.

Funding

This work was supported by the Minnesota Lions Vision Foundation.

Authorship

All authors attest that they meet the current ICMJE criteria for Authorship.

Declaration of competing interest

The Authors declare that there is no conflict of interest.

Acknowledgements

An abstract and a poster of this manuscript have been presented at The Association for Research in Vision and Ophthalmology 2016 Meeting, Seattle WA, on May 1, 2016.

Appendix A. Supplementary data

Supplementary data to this article can be found online at <https://doi.org/10.1016/j.ajoc.2020.100666>.

References

1. McCannel CA, Berrocal AM, Holder GE, et al. *Basic and Clinical Science Course Section*

12. *Retina and Vitreous*. 2019-2020 San Francisco: Amer. Acad. Ophthalmol; 2019:327–328.
2. Elsner AE, Burns SA, Weiter JJ, et al. Infrared imaging of sub-retinal structures in the human ocular fundus. *Vision Res*. 1996;36:191e205.
3. Schmitz-Valckenberg S, Holz FG, Bird AC, Spaide RF. Fundus autofluorescence imaging: review and perspectives. *Retina*. 2008;28(3):385–409.
4. De Zaeytjyd J, Vanakker OM, Coucke PJ, De Paepe A, De Laey JJ, Leroy BP. Added value of infrared, red-free and autofluorescence fundus imaging in pseudoxanthoma elasticum. *Br J Ophthalmol*. 2010;94(4):479–486.
5. Ho VY, Wehmeier JM, Shah GK. Wide-field infrared imaging: a descriptive review of characteristics of retinoschisis, retinal detachment, and schisis detachments. *Retina*. 2016;36(8):1439–1445.
6. Ip M, Garza-Karren C, Duker JS, et al. Differentiation of degenerative retinoschisis from retinal detachment using optical coherence tomography. *Ophthalmology*. 1999;106(3):600–605.
7. Nagrao S, Gaitan JR, Flynn Jr HW, Smiddy WE. Optical coherence tomography findings in patients with degenerative retinoschisis and symptomatic retinal detachment. *Ophthalm Surg Lasers Imag Retina*. 2010;42:E1–E5.
8. Stehouwer M, Tan SH, van Leeuwen TG, Verbraak FD. Senile retinoschisis versus retinal detachment, the additional value of peripheral retinal OCT scans (SL SCAN-1, Topcon). *Acta Ophthalmol*. 2014;92(3):221–227.
9. Xiao W, Zhu Z, Odouard C, Xiao O, Guo X, He M. Wide-field en face swept-source optical coherence tomography features of extrafoveal retinoschisis in highly myopic eyes. *Invest Ophthalmol Vis Sci*. 2017;58(2):1037–1044.
10. Choudhry N, Golding J, Manry MW, Rao RC. Ultra-widefield steering-based spectral-domain optical coherence tomography imaging of the retinal periphery. *Ophthalmology*. 2016;123(6):1368–1374.
11. Salvanos P, Navaratnam J, Ma J, Bragadóttir R, Moe MC. Ultra-widefield autofluorescence imaging in the evaluation of scleral buckling surgery for retinal detachment. *Retina*. 2013;33(7):1421–1427.
12. Witmer MT, Cho M, Favarone G, Chan RV, D'Amico DJ, Kiss S. Ultra-wide-field autofluorescence imaging in non-traumatic rhegmatogenous retinal detachment. *Eye*. 2012;26(9):1209–1216.
13. Lois N, Forrester J. *Fundus Autofluorescence*. Philadelphia, PA: Lippincott Williams and Wilkins; 2009.
14. Sekiryu T, Oguchi Y, Arai S, Wada I, Iida T. Autofluorescence of the cells in human subretinal fluid. *Invest Ophthalmol Vis Sci*. 2011;52(11):8534–8541.
15. Sayanagi K, Ikuno Y, Tano Y. Different fundus autofluorescence patterns of retinoschisis and macular hole retinal detachment in high myopia. *Am J Ophthalmol*. 2007;144:299–301.
16. Hiraoka T, Inoue M, Ninomiya Y, Hirakata A. Infrared and fundus autofluorescence imaging in eyes with optic disc pit maculopathy. *Clin Exp Ophthalmol*. 2010;38(7):669–677.